Aerosol and Air Quality Research, 14: 1431–1442, 2014

ISSN: 1680-8584 print / 2071-1409 online
doi: 10.4209/aaqr.2013.06.0203

Characteristics of Aerosol Optical Properties and Their Chemical Apportionments during CAREBeijing 2006

Tingting Han[1], Xingang Liu[1*], Yuanhang Zhang[2*], Yu Qu[3], Jianwei Gu[2], Qiang Ma[1], Keding Lu[2], Hezhong Tian[1], Jing Chen[1], Limin Zeng[2], Min Hu[2], Tong Zhu[2]

[1] *State Key Laboratory of Water Environment Simulation, School of Environment, Beijing Normal University, Beijing 100875, China*
[2] *State Key Joint Laboratory of Environment Simulation and Pollution Control, College of Environmental Sciences and Engineering, Peking University, Beijing 100871, China*
[3] *State Key Laboratory of Atmospheric Boundary Layer Physics and Atmospheric Chemistry, Institute of Atmospheric Physics, Chinese Academy of Sciences, 100029, China*

ABSTRACT

Field campaigns monitoring the aerosol optical properties and chemical components of PM_{10} were carried out in Beijing in 2006 summer. The average light extinction coefficient b_{ext}, dry aerosol scattering coefficient b_{sp} and aerosol absorption coefficient b_{ap} were 895.0 ± 820.8 Mm^{-1}, 364.0 ± 324.3 Mm^{-1} and 57.8 ± 31.1 Mm^{-1}, respectively. b_{ext}, b_{sp} and b_{ap} had the similar increasing trend during the formation process of haze. Pronounced diurnal cycles were observed for ω_{550} (aerosol single scattering albedo at 550 nm), b_{sp}, b_{ap} and b_{ext}. The dry b_{sp} was elevated during the daytime with a maximum mean value of 475.8 Mm^{-1} (LST 06:00). b_{ext}, $PM_{2.5}$ mass concentration and $PM_{2.5}/PM_{10}$ ratio increased at night due to continuous emissions of pollutants to the lower nocturnal boundary layer, and decreased during the daytime due to convective mixing. b_{ap} increased at night, and decreased during the daytime and reached the minimum (37 Mm^{-1}) at LST 16:00. The single scattering albedo reached its maximum (0.87) at LST 11:00. This trend was consistent with the SNA (sulfate, nitrate, and ammonium)/PM_{10} ratio and was contrary to the BC (black carbon)/PM_{10} ratio, which demonstrated that secondary pollution largely influenced the scattering ability of aerosols. Ammonium sulfate, ammonium nitrate, organic mass, elemental carbon and coarse mass contributed 26.5%, 15.2%, 21.8%, 16.1% and 20.4% to the total extinction coefficient during clean days, and 44.6%, 22.3%, 13.6%, 10.8% and 8.7% during hazy days. The fractional contributions of ammonium sulfate and ammonium nitrate were significantly higher during the hazy time than those during the clean days. While the fractional contributions of organic mass, elemental carbon and coarse mass were lower during the haze time than those during the clean days.

Keyword: Optical properties; Diurnal variations; Chemical apportionment; Beijing.

INTRODUCTION

Atmospheric aerosols, consisting of liquid and solid particles suspended in the air, are important components of atmosphere. Aerosols play a significant role in visibility reduction (Watson, 2002), regional air quality (Molina and Molina, 2004), and climate change (IPCC, 2007). Components of airborne aerosols, such as sulfate, nitrate, ammonium, black carbon (BC), particulate organic matter (POM), and other chemical species can scatter and absorb the incident light and therefore lead to atmospheric dimming and horizontal visibility degradation (Liu *et al.*, 2009). Several key aerosol optical properties (AOPs), including atmospheric aerosol burden, single scattering albedo (ω), upscatter fraction and the mass scattering and absorption efficiencies must be measured or estimated to evaluate the local or regional aerosol pollution (Chýlek and Wong 1995). To fully understand the aerosol optical properties, extensive sets of both in situ and remote measurements are required (Alados-Arboledas *et al.*, 2008). Several observational networks of aerosol optical properties have been established internationally including AERONET (AErosol RObotic NETwork), SKYNET (SKY Network), AEROCAN (Canadian Sunphotometer Network), RIMA (Red Ibérica de Medida de Aerosoles), AGSNet (Aerosol Ground Station Network) and others (Holben *et al.*, 1998; Bokoye *et al.*, 2001; O'Brien and Mitchell, 2003; Uchiyama *et al.*, 2005; Campanelli *et al.*, 2007; Goloub *et al.*, 2008).

Previous studies showed that sulfate and organic mass are the main chemical components contributing to light

* Corresponding author.
E-mail address: liuxingang@bnu.edu.cn (X. Liu); yhzhang@pku.edu.cn (Y. Zhang)

extinction and visibility degradation (Cheung *et al.*, 2005; Yuan *et al.*, 2006; Yang *et al.*, 2007; Tao *et al.*, 2009; Liu *et al.*, 2012). Though gas pollutants can also reduce visibility through light extinction, this influence is generally weak (Chan *et al.*, 1999). Moreover, meteorological parameters also contribute to visibility degradation, especially relative humidity (Malm and Day, 2001; Liu *et al.*, 2008; Liu *et al.*, 2013a, b). Many studies on chemical compositions of PM_{10} (particulate matter with aerodynamic diameter less than 10 μm) and $PM_{2.5}$ (particulate matter with aerodynamic diameter less than 2.5 μm) in Beijing have been carried out during last decade (He *et al.*, 2001; Yao *et al.*, 2002; Yang *et al.*, 2005; Sun *et al.*, 2006). These studies indicated that the water soluble inorganic ions and carbonaceous aerosols were major components of aerosols. There are also studies focusing on pollution levels and chemical compositions such as water soluble inorganic ions, carbonaceous fractions, and trace elements (He *et al.*, 2001; Ye *et al.*, 2003; Duan *et al.*, 2006; Gu *et al.*, 2011), however, studies on the relationship between aerosol chemical composition and optical properties remain limited. Thus, it is necessary to study the characteristics of aerosol optical properties and their chemical apportionments to understand the cause of visibility degradation. In this study, we analyzed the chemical components and optical properties of aerosols from 18 August to 8 September 2006 in the urban area of megacity Beijing, and studied the relations between aerosol optical properties and their chemical components.

EXPERIMENT

Experiment Site

The CAREBeijing 2006 campaign (Liu *et al.*, 2009) was carried out in urban and rural site of Beijing, China in the summer of 2006. By the end of 2006, Beijing had a population of 15.8 million with a population density of 963 people per square kilometer (http://www.bjstats.gov.cn/nj/main/2007-tjnj/index.htm). With the rapid economic growth (annual GDP had a growth rate of 12.8% in 2006), the total energy consumption reached 59 million tons of standard coal (http://www.bjstats.gov.cn/nj/main/2007-tjnj/index.htm). The number vehicles also reached 2.8 million in 2006, an increase of 11.9% compared with 2005 (http://www.bjstats.gov.cn/nj/main/2007-tjnj/index.htm). High population density and extensive economic activities had inevitably resulted in heavy emission of air pollutants in Beijing.

Field measurements in urban site of Beijing were carried out from August 18 to September 8, 2006 on the campus of Peking University (39.98°N, 116.35°E), which is located in the north-western of Beijing and is ~600 meters to the north fourth ring road. The observation station was set up on the roof of a 6-floor building (~20 m above ground level). The observation sites are to some extent influenced by local vehicular traffic, combustion of fuels for cooking, local industrial activities and some of transported pollutants (Liu *et al.*, 2009).

Measurement and Method

Instruments used in this study with their model and manufacturer information are listed in Table 1. Mass concentrations of PM_{10} and $PM_{2.5}$ were measured by the dust monitors & counters (Grimm M265, USA). Water-soluble ionic components (WSIC) including cations (Na^+, NH_4^+, K^+, Mg^{2+}, Ca^{2+}) and anions (Cl^-, NO_2^-, NO_3^-, SO_4^{2-}) in PM_{10} were measured by an in-situ particle-into-liquid sampler (PILS) system (Orsini *et al.*, 2003). Atmospheric extinction coefficient b_{ext}, aerosol scattering coefficient at dry conditions b_{sp}, aerosol absorption coefficient b_{ap}, and RH were measured by transmissiometer (Malm and Persha, 1991), integrating nephelometer (Anderson and Ogren, 1998), multi-angle absorption photometer (MAAP) (Petzold and Schonlinner, 2004), and automatic meteorological station, respectively. It should be noted that the wavelengths that the optical instruments used were different. As a result, all parameters were scaled to values at the wavelength of 550 nm by using power-law wavelength dependence (Liu *et al.*, 2012). Elemental carbon (EC) and organic carbon (OC) were monitored by a semi-continuous OC/EC analyzer with the thermal-optical transmittance method (Kondo *et al.*, 2006). Mie scattering LIDAR (light detection and ranging), being

Table 1. Instruments for atmospheric aerosol optical properties and chemical components at PKU in summer 2006.

Parameters	Instrument	Model	Calibration	Wavelength (nm)	Resolution
Light extinction coefficient (b_{ext})	transmissometer	LPV-2 Optec, USA	Before and after the campaign	550	1 min
Aerosol scattering coefficient (b_{scat})	Nephelometer	M9003 Ecotech, Australia	Before and after the campaign	525	5 min
Aerosol absorption coefficient (b_{abs})	MAAP	5012 Thermo Scientific	Before and after the campaign	670	1 min
PM_{10}, $PM_{2.5}$ mass concentration	Dust monitors & counters	GRIMM 265	/	/	30 min
Organic carbon/elemental carbon(OC/EC)	Semi-continous OC/EC analyzer	Sunset Laboratory, Oregon, USA	/	/	1 hour
Water-soluble ions	PILS system	Dionex, USA	Zero check every day	/	15 min
Height of PBL	LIDAR	Mie Compact	/	532/1064	15 min

similar to that reported by Sugimoto *et al.* (2009), continuously monitored the profile of aerosol distribution in troposphere. We used the coefficient of variance (v) of LIDAR signals calculated by Eq. (1) to determine the height of the PBL (planetary boundary layer) (Liu *et al.*, 2013b; Strawbridge and Snyder, 2004).

$$v = \frac{S}{\bar{x}} \times 100\% = \frac{\sqrt[n]{\frac{\sum_{i=1}^{n}(x_i - \bar{x})^2}{n}}}{\sum_{i=1}^{n} x_i} \times 100\% \quad (1)$$

where S is standard deviation and $\bar{x}$ is the average of adjacent five LIDAR signals, which were from the normalized backscattering data on 532 nm wavelength channel. The site where its coefficient of variance is the maximum is the height of the PBL.

All of the instruments mentioned above were calibrated according to their manufacturers' manual. The transmissiometer was installed outdoor, and other instruments were installed in an air-conditioned room.

The light extinction coefficient, b_{ext}, which is wavelength dependent, can be expressed as the sum of scattering (b_{scat}) and absorption (b_{abs}) by Eq. (2).

$$b_{ext} = b_{scat} + b_{abs} = b_{sg} + b_{sp} + b_{ag} + b_{ap} \quad (2)$$

where b_{scat} is the sum of scattering by gases b_{sg} and particles b_{sp}, and b_{abs} is the sum of absorption by gases b_{ag} and particles b_{ap}. b_{sg} is referred to as Rayleigh scattering (approximately 10 Mm^{-1}), and b_{sp}, which is the largest contributor to total light extinction in most areas (Malm *et al.*, 1994; Chan *et al.*, 1999), is caused by both fine and coarse particles. b_{ag} is mainly due to absorption of nitrogen dioxide (NO_2), while b_{ap} is primarily caused by carbon-containing particles.

The approach used in the IMPROVE (The Interagency Monitoring of Protected Visual Environments) program to estimate light extinction for aerosol components assumes externally mixed aerosols. The reconstructed b_{ext} can then be calculated from the mass concentrations of the aerosol components using Eq. (3), based on the original IMPROVE algorithm (Malm and Hand, 1994; Malm *et al.*, 2007):

$$b_{ext} = 3f(RH) \times [(NH_4)_2SO_4] + 3f(RH) \times [NH_4NO_3] + 4 \times [POM] + 10 \times [EC] + 1 \times [Fine\ Soil] + 0.6 \times [Coarse\ Mass] + 0.161 \times [NO_2] + 10 \quad (3)$$

$$[(NH_4)_2SO_4] = 0.944 \times [NH_4^+] + 1.02 \times [SO_4^{2-}] \quad (4)$$

$$[NH_4NO_3] = 1.29 \times [NO_3^-] \quad (5)$$

$$[POM] = 1.6 \times [OC] \quad (6)$$

$$[Fine\ Soil] = 2.49 \times [Si] + 2.2 \times [Al] + 2.42 \times [Fe] + 1.63 \times [Ca] + 1.94 \times [Ti] \quad (7)$$

$$[Coarse\ Mass] = PM_{10} - PM_{2.5} \quad (8)$$

Eq. (3) includes a constant 10 Mm^{-1} which denotes the Rayleigh scattering of clear air. The light extinction coefficients of atmospheric aerosol are in Mm^{-1}. The chemical composition concentrations shown in brackets are in unit of $\mu g/m^3$. Dry efficiency terms are in unit of m^2/g; and the hygroscopic growth terms, f(RH), are unitless. Elemental carbon (EC) is referred to as light absorbing carbon (b_{ap} = 10[EC]), and the mass extinction coefficient of hygroscopic aerosol implies a RH-dependent scaling factor (f(RH)), which represents the relationship between RH and the scattering efficiency. Eqs (4) and (5) assume that SO_4^{2-} and NO_3^- are fully neutralized by NH_4^+. Particulate organic matter (POM) was estimated by multiplying the measured OC by a factor (1.6) to compensate for other atoms such as H, O and N in the organic molecule (Turpin and Lim, 2001).

RESULTS AND DISCUSSION

Temporal Variations of Aerosol Chemical and Optical Properties

Temporal variations of the chemical components, optical properties of aerosols and ambient visibility in Beijing from August 18 to September 8 are depicted in Fig. 1. According to the definition of haze (visibility < l0 km and RH < 90%) (Wu *et al.*, 2006), there were four haze episodes observed in Beijing in the time periods of Aug. 18 0:00–Aug. 20 06:00, Aug. 23 1:00–Aug. 28 22:00, Aug. 31 17:00–Sep. 03 11:00 and Sep. 05 22:0–Sep. 08 3:00, and the other days during the campaign could be classified to clean day. b_{ext}, b_{sp} under dry condition and b_{ap} had the similar trend to increase during the formation process of haze. The maximum value of b_{ext}(RH) was nearly 5100 Mm^{-1} in the morning of 25th August and the corresponding visibility was as low as 0.8 km. Similarly, the mass concentrations of SO_4^{2-}, NO_3^-, NH_4^+ and POM also showed an upward trend during the process of haze formation. The average concentrations of SO_4^{2-}, NO_3^-, NH_4^+ and POM were 49.8, 31.4, 25.8 and 25.0 $\mu g/m^3$ during the haze episodes in Beijing, which greatly exceeded the overall average of these components during the whole campaign, (34.8, 24.5, 20.7 and 20.9 $\mu g/m^3$) and even more greater than those during the clean day (11.7, 9.2, 6.3 and 13.9 $\mu g/m^3$). The mass concentrations of SO_4^{2-}, NO_3^-, NH_4^+ and POM in hazy days were 4.3, 3.4, 4.1, and 1.8 times of those in clean days. Similar high ratios for NO_3^-, SO_4^{2-}, and NH_4^+ in $PM_{2.5}$ between haze days and clean days (6.5, 3.9, and 5.3) have been observed in Guangzhou city of China (Tan *et al.*, 2006). The atmospheric extinction coefficient, dry aerosol scattering coefficient and aerosol absorption coefficient at 550 nm during CAREBeijing-2006 for b_{ext}, b_{sp} and b_{ap} were 895.0 ± 820.8 Mm^{-1}, 364.0 ± 324.3 Mm^{-1} and 57.8 ± 31.1 Mm^{-1}, respectively. Bergin *et al.* (2001) reported $b_{sp,530}$ = 488 ± 370 Mm^{-1} and $b_{ap,565}$ = 83 ± 40 Mm^{-1} from a one-week intensive campaign in June 1999 also on the campus of Peking University. Li *et al.* (2007) reported $b_{sp,550}$ = 468 ± 472 Mm^{-1} and $b_{ap,550}$ = 65 ± 75 Mm^{-1} in March 2005 at rural Xianghe (~70 km southeast of Beijing). The results of this study are smaller than those reported from urban Guangzhou ($b_{sp,545}$ = 463 ± 178 Mm^{-1} and $b_{ap,532}$ = 92 ± 62 Mm^{-1}) (Andreae *et al.*, 2008), but are similar to those in the Yangtze

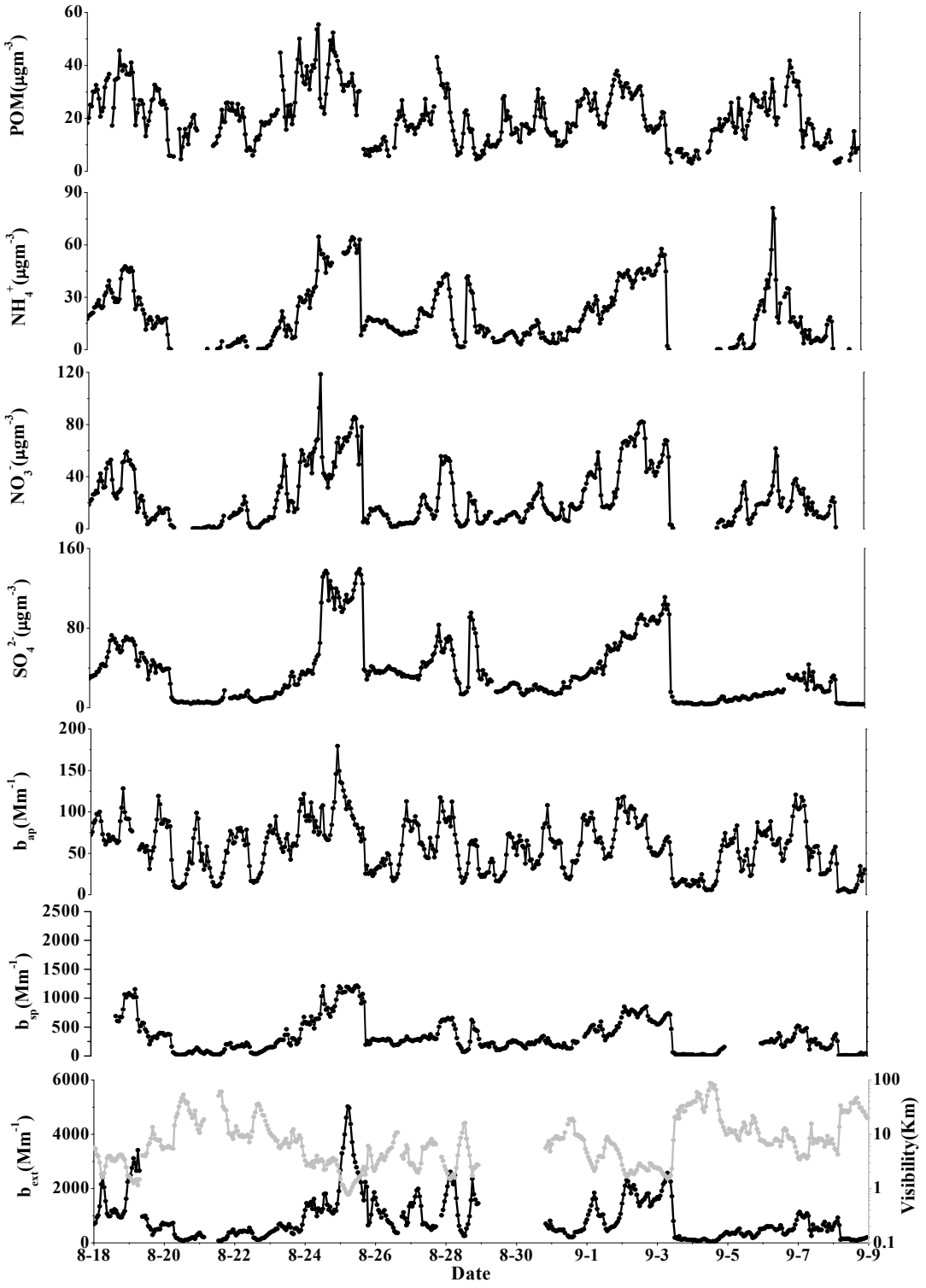

Fig. 1. Time series of the optical parameters (b_{ext}, b_{sp}, b_{ap}), Visibility, and mass concentrations of the chemical components.

delta ($b_{sp,530}$ = 353 ± 202 Mm^{-1} and $b_{ap,565}$ = 23 ± 14 Mm^{-1}) (Xu *et al.*, 2002) as well as southeast of Guangzhou in Xinken ($b_{sp,550}$ = 333 ± 138 Mm^{-1} and $b_{ap,550}$ = 70 ± 42 Mm^{-1}) (Cheng *et al.*, 2008). While the current study's results are larger than a study carried out at a rural site about 150 km northeast of Beijing ($b_{sp,525}$ = 174.6 ± 189.1 Mm^{-1}) (Yan *et al.*, 2008) as well as a study ~60 km northwest of Guangzhou ($b_{sp,550}$ = 151 ± 103 Mm^{-1} and $b_{ap,532}$ = 34.3 ± 26.5 Mm^{-1}) (Garland*et al.*, 2008). Overall, the average scattering and absorption coefficients observed in this study were higher than reported from other suburban areas but lower than those typically measured in the urban areas of Chinese megacities.

The frequency distributions of dry scattering coefficient, extinction coefficient, absorption coefficient and single

scattering albedo in Beijing are shown in Fig. 2. The frequency distributions of absorption coefficient and single scattering albedo ω (section 3.2) at 550 nm were essentially normal distributed. The mean (μ) and variance (δ) values of absorption coefficient were 54.4 Mm^{-1} and 41.1 Mm^{-1}, and corresponding values of single scattering albedo were 0.84 and 0.07. As can be seen from the Fig. 2, nearly 59% of the absorption coefficient values located in the range of 40~100 Mm^{-1}, while approximately 82% of the single scattering albedo values focused on the range of 0.7–1.0. In spite of this, the frequency distribution of dry scattering coefficient and extinction coefficient were different, that is, most of the dry scattering coefficient and extinction coefficient was distributed in the lower range. Obviously, there were 68% of the dry scattering coefficient values concentrated on the limits of 0–400 Mm^{-1} and 66% of the extinction coefficient values located in the range of 0–1100 Mm^{-1}.

Diurnal Variations of the Optical Properties and Their Chemical Apportionments

Time series of optical properties shown in Fig. 1 already suggested the existence of significant diel trends. These are confirmed further by plots of hourly averages (Fig. 3). Fig. 3 illustrates the diurnal variations of dry b_{sp}, b_{ap}, b_{ext} and ω, respectively. The dry b_{sp} was elevated during the daytime with a maximum mean value of 475.8 Mm^{-1} (LST 06:00). Then, the mean values descended between LST 08:00 and LST 20:00 with a minimum mean value of 120 Mm^{-1} (LST 20:00). Fig. 3(b) displayed the diurnal cycle of b_{ap}, which was even more pronounced than that of dry b_{sp}. Apparently, from LST 06:00 to LST 16:00, the mean b_{ap} values continuously declined and reached the minimum (37 Mm^{-1}) at LST 16:00 before it began to increase. The maximum mean value of b_{ap} was 80 Mm^{-1} at LST 23:00. For the diurnal variation of extinction coefficient, the first peak of b_{ext} occurred at LST 06:00 and the second peak appeared at LST 18:00, which indicated that the extinction coefficient increased with the deterioration of air pollution during the morning and evening traffic peak. The single scattering albedo, ω_λ, is the ratio of the scattering coefficient over the extinction coefficient at a given wavelength. Here ω has been calculated at λ = 550 nm using Eq. (9).

$$\omega_{550} = \frac{b_{sp}}{b_{sp} + b_{ap}} \tag{9}$$

The single scattering albedo reflects the scattering power of the atmospheric particulate matter. The mean and standard deviation for ω_{550} for the campaign was 0.80 ± 0.11, which is close to the values reported from other locations in and around Beijing and Guangzhou for the single scattering albedo of dry aerosol particles in the green spectral range [ω = 0.82–0.85 (Li *et al.*, 1993; Bergin *et al.*, 2001; Cheng *et al.*, 2008; Garland *et al.*, 2008; Andreae *et al.*, 2008)]. It indicated a bigger proportion of absorbing particulate matter at the urban site. As shown in Fig. 3(d), there were two peaks and two valleys. The major peak occurred at

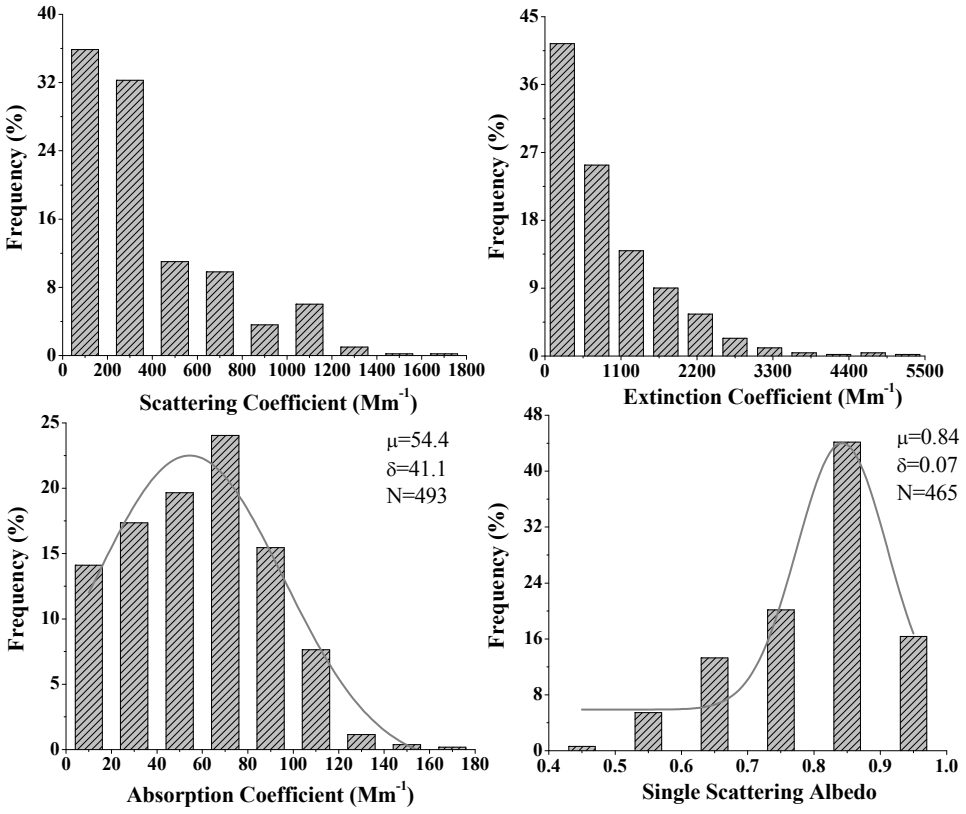

Fig. 2. The frequency distribution of scattering coefficient (b_{sp}), extinction coefficient (b_{ext}), absorption coefficient (b_{ap}) and single scattering albedo (SSA) in Beijing.

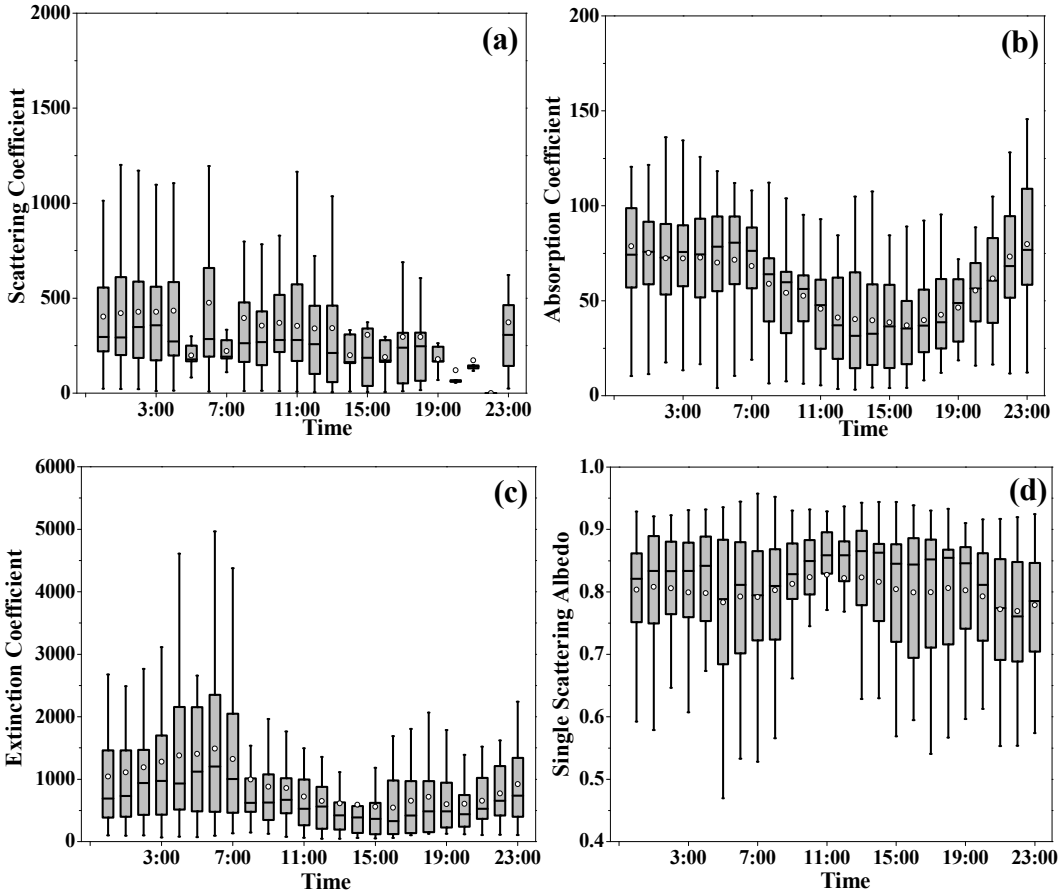

Fig. 3. Diurnal variations of (a) b_{sp}; (b) b_{ap}; (c) b_{ext} and (d) SSA (Single Scattering Albedo) in Beijing. The dot is the mean value, the horizontal line in the box is the median, the limits of the boxes are the 25th percentile and 75th percentile, and the vertical lines extend to 5th and 95th percentiles for each 1-h period after the indicated start time.

LST 11:00, and the other peak was at LST 18:00. The two valley values appeared at LST 05:00 (0.78) and LST 16:00 (0.79), respectively.

For comparison, Fig. 4 displays the diurnal cycles of the $PM_{2.5}$ mass concentration, $PM_{2.5}/PM_{10}$ ratio, SNA/PM_{10} ratio, BC/PM_{10} ratio and the height of PBL, respectively. In Beijing, higher $PM_{2.5}$ concentrations were observed in the night and maximum values observed at LST 23:00 and LST 0:00. $PM_{2.5}$ concentrations began to decrease from LST 0:00 to LST 5:00 except a little peak at LST 6:00. $PM_{2.5}$ concentrations kept on decreasing until LST 16:00, then, $PM_{2.5}$ concentrations started to increase. The trend of $PM_{2.5}/PM_{10}$ ratio was similar with the $PM_{2.5}$ mass concentrations which corresponding to the diurnal variations of b_{ext}. The diurnal cycles of b_{ext}, $PM_{2.5}$ mass concentrations and $PM_{2.5}/PM_{10}$ ratio were possibly dominated by convective mixing during the daytime, leading to a dilution and thus a decrease. After sunset, the formation of a stable nocturnal boundary layer (BL) in combination with the continued emission or advection of particles and gases throughout the night, leads to an increase in b_{ext}, $PM_{2.5}$ mass concentration and $PM_{2.5}/PM_{10}$ ratio. Low height of BL would retain the pollutants in the surface layer (Liu *et al.*, 2013). The diurnal variation of the height of PBL is displayed in the Fig. 4(e). The height of PBL rose from LST 8:00 and reached its peak at LST 14:00, then gradually decreased until LST 23:00. Obviously, the diurnal variation of PBL showed an opposite trend with the mass concentration of $PM_{2.5}$. Because the b_{ap} was calculated from the mass concentration of BC, the diurnal variation of BC/PM_{10} ratio was consistent with b_{ap}. Lastly, the SNA/PM_{10} ratio was elevated during the daytime with a maximum mean value of 0.5 at LST 12:00. The SNA/PM_{10} ratio increased with the height of PBL rising during noon time, which indicated that secondary transformation of SNA was active in the noon. Both the mean and median values then decreased between LST 12:00 and LST 21:00 with a minimum mean value of 0.38 at LST 21:00. This trend was consistent with the SSA, which implied that secondary pollution would largely influence the scattering ability of aerosols and the chemical composition had an important impact on the optical properties. As for the reason why SSA reached the maximum at midday, it was partly due to the strong photochemical reactions that led to the formation of secondary pollutant with strong scattering and negligible absorption ability. Meanwhile, the lowest value of BC/PM_{10} ratio was observed at midday. The sulfur oxidation ratio ($SOR = nSO_4^{2-}/(nSO_4^{2-} + nSO_2)$, where n refers to the molar concentration) and the nitrogen oxidation ratio ($NOR = nNO_3^-/(nNO_3^- + nNO_2)$) are good indicators of secondary transformation. The higher values of SOR and NOR

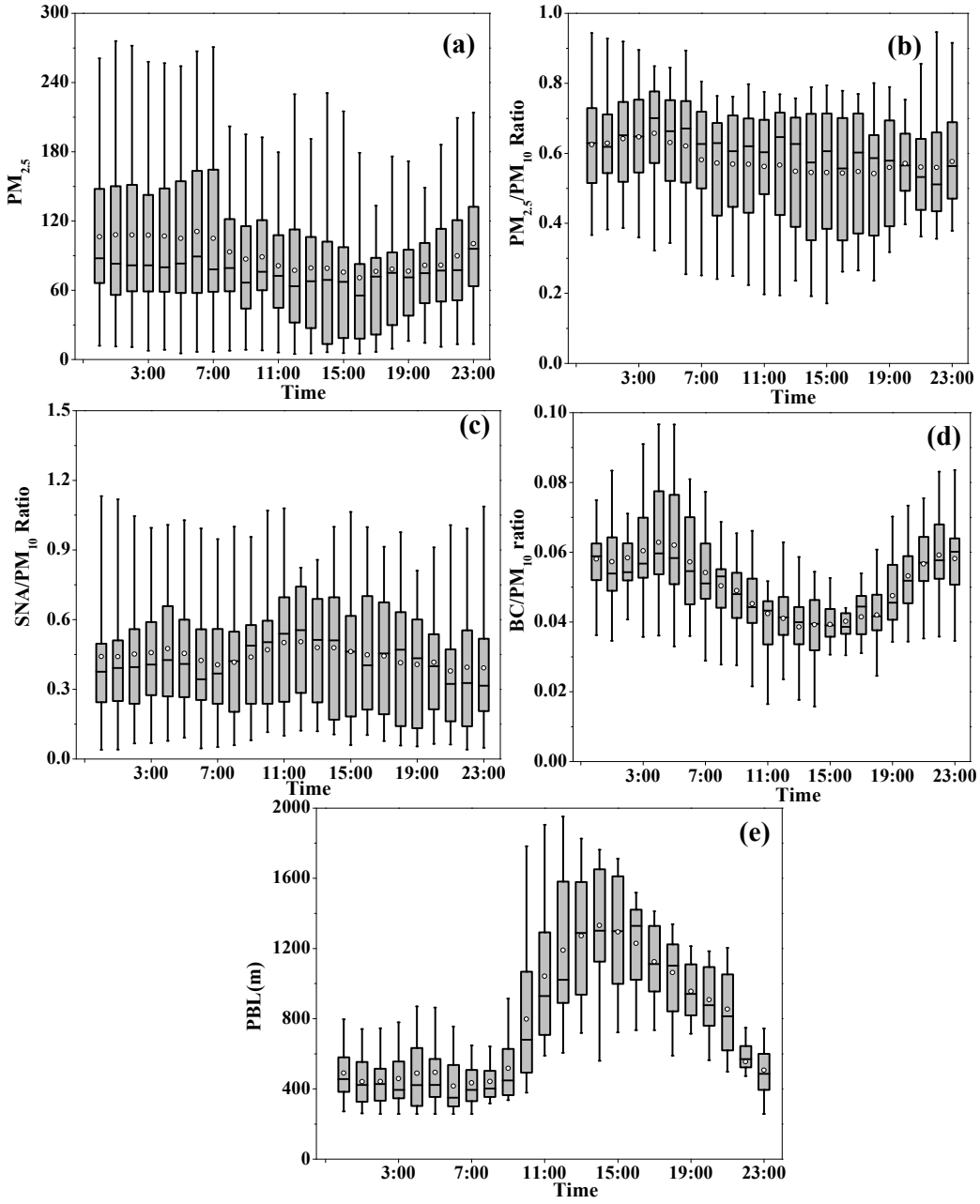

Fig. 4. Diurnal variations of the (a) $PM_{2.5}$ mass concentration; (b) $PM_{2.5}/PM_{10}$ ratio; (c) SNA (sulfate, nitrate, and ammonium)/PM_{10} ratio and (d) BC/PM_{10} ratio in Beijing ; (e) The height of PBL (m). Symbols are analogous to Fig. 3.

indicated that more gaseous species had been oxidized to secondary aerosol in the atmosphere (Sun *et al.*, 2006). The diurnal variations of SOR and NOR are depicted in Fig. 5, where a small peak of SOR and NOR was observed at LST 11:00 which conformed to the influence of secondary pollutants to SSA.

Chemical Apportionment of the Aerosol Optical Properties

Figs. 6(a), 6(b) and 6(c) illustrate the relationship between b_{sp}, b_{ap}, b_{ext} and the mass concentration of $PM_{2.5}$ in Beijing during the whole campaign, respectively. In Fig. 6(c), b_{ext} showed an strong and positive correlation with $PM_{2.5}$ mass concentration with a correlation coefficient of 0.90. As shown in Fig. 6(b), b_{ap} was also strong correlated (r = 0.95) with $PM_{2.5}$ mass concentration. Same strong correlation was observed for b_{sp} and $PM_{2.5}$ mass concentration.

In this study, we mainly studied the extinction effect by fine particles and the contribution of fine soil was excluded in b_{ext} estimation because it only accounted for a small fraction of $PM_{2.5}$ mass (Wang, 2003). Extinction by fine soil could be neglected from the standpoint of light extinction in summer in Beijing (Liu *et al.*, 2009). Thus, the modified IMPROVE algorithm is presented as Eq. (10).

$$b_{ext} \approx 3f(RH) \times [(NH_4)_2SO_4] + 3f(RH) \times [NH_4NO_3] + 4 \times [POM] + 10 \times [EC] + 0.6 \times [Coarse\ Mass] + 10 \quad (10)$$

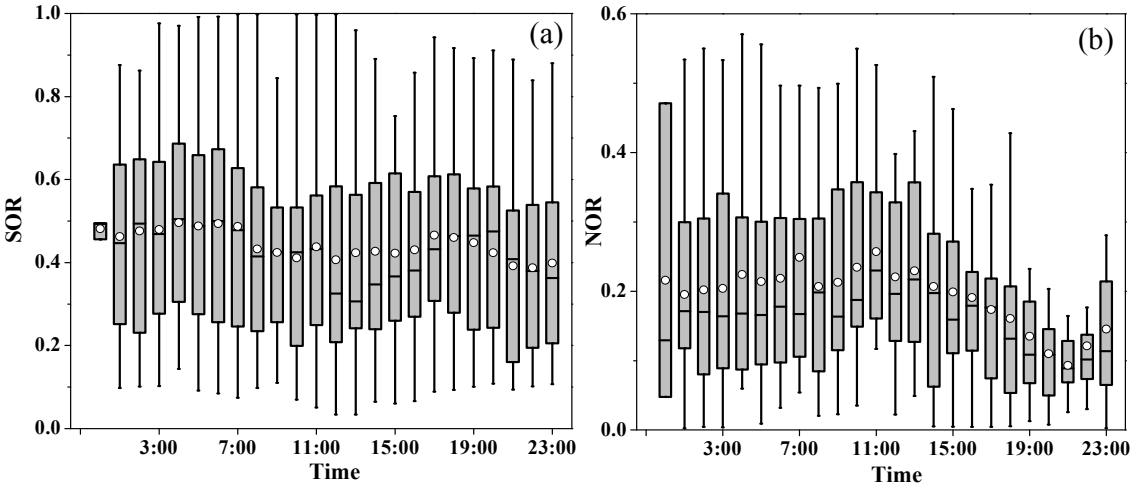

Fig. 5. Diurnal variations of the (a) SOR (sulfur oxidation ratio) and (b) NOR (nitrogen oxidation ratio) in Beijing. Symbols are analogous to Fig. 3.

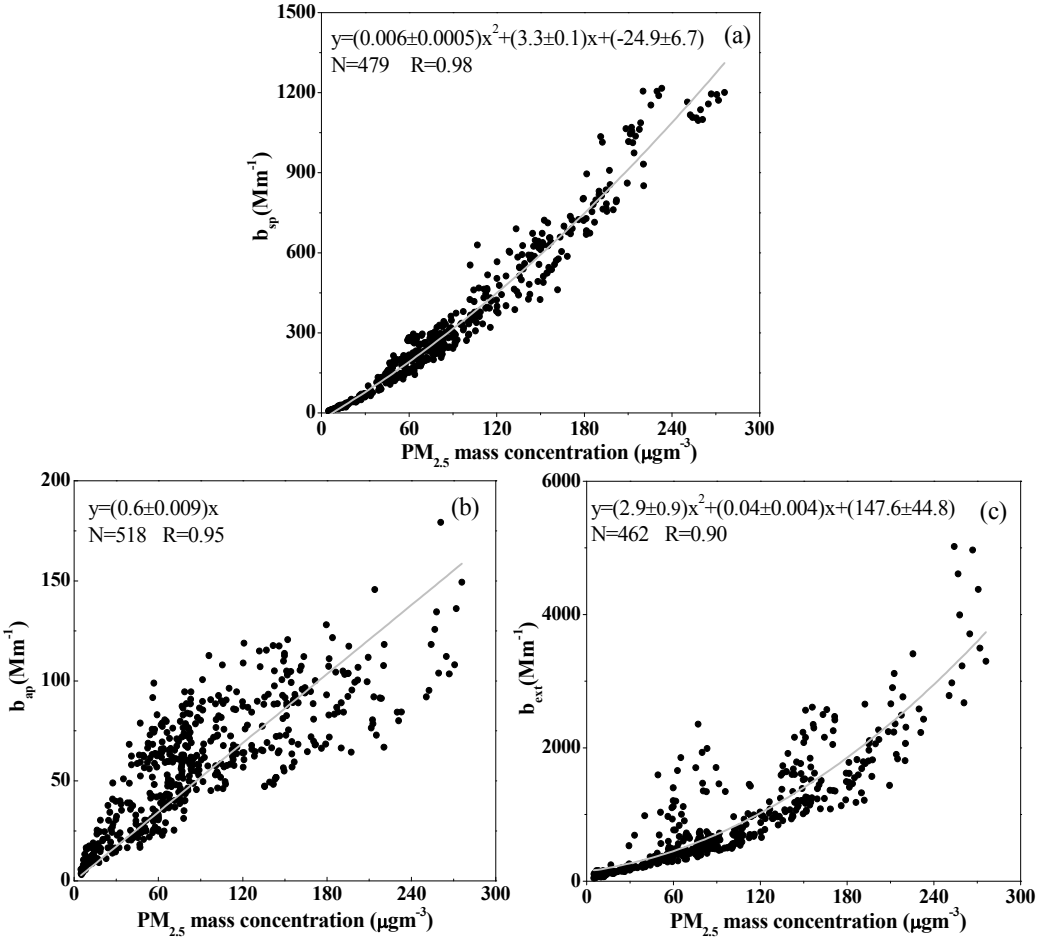

Fig. 6. Relationship between the mass concentration of $PM_{2.5}$ and (a) b_{sp}; (b) b_{ap}; (c) b_{ext} in Beijing.

Table 2 summarizes different f(RH) values for $(NH_4)_2SO_4$ and NH_4NO_3 in selected relative humidity ranges (Malm and Day, 2001; Liu *et al.*, 2012). Table 3 lists the composite variables for particulate matter proposed by IMPROVE. According to the Eqs. (4), (5), (6), (8) and (10), the calculated b_{ext} can be derived and then compared with the measured b_{ext}. As depicted by Fig. 7(a), the measured b_{ext} were slightly larger than the calculated b_{ext} and the deviation between measured values and calculated values was about 18.4%. Fig. 7(b) illustrated that the correlation coefficient between

Table 2. Statistical summary of mean f(RH) values for $(NH_4)_2SO_4$ and NH_4NO_3 in selected relative humidity ranges.

RH (%)	20–25	25–30	30–35	35–40	40–45	45–50	50–55	55–60	60–65	65–70	70–75	75–80	80–85	85–90	> 90
f (RH)	1.06	1.11	1.16	1.21	1.22	1.27	1.33	1.38	1.45	1.55	1.65	1.83	2.10	2.46	3.17

Table 3. Composite variables for particulate matter proposed by IMPROVE.

Component	Specification	Mass calculation
$(NH_4)_2SO_4$	Ammonium sulfate	$0.944[NH_4^+] + 1.02[SO_4^{2-}]$[a]
NH_4NO_3	Ammonium nitrate	$1.29[NO_3^-]$
OMC	Organic mass by carbon	1.6[OC][b]
b_{abs}	Absorption coefficient	[EC]
CM	Coarse mass	$[PM_{10}]$-$[PM_{2.5}]$

[a] Malm and Day, 2001; Tao *et al.*, 2009.
[b] Turpin and Lim, 2001.

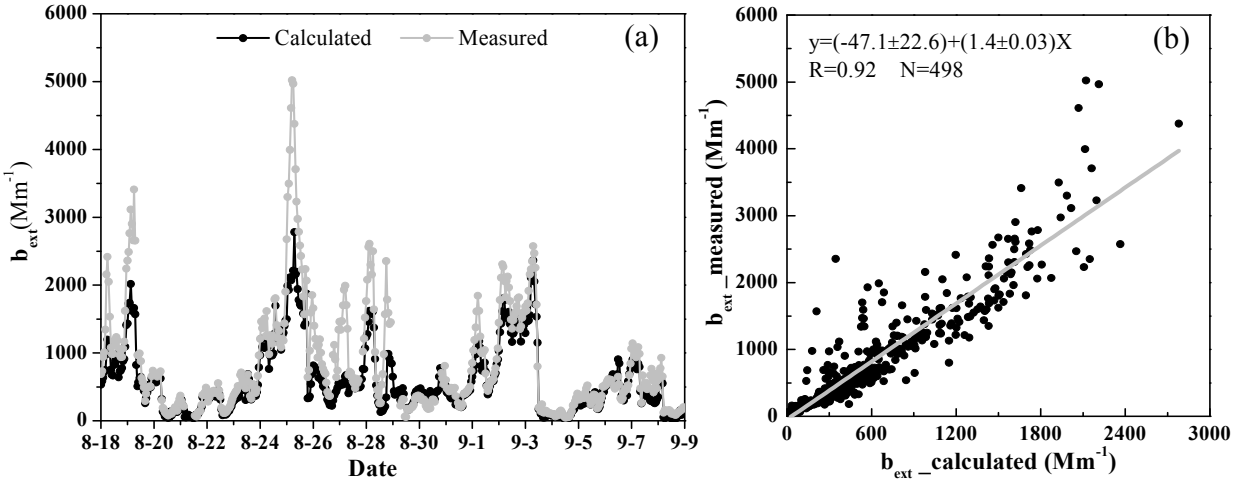

Fig. 7. (a) Time series of the measured b_{ext} and the calculated b_{ext} in Beijing; (b) Relationship between the measured b_{ext} and the calculated b_{ext}.

measured b_{ext} and calculated b_{ext} was 0.92, which verified the reliability of IMPROVE algorithm. We conclude that IMPROVE Eq. (10) can be used to calculate the chemical apportionment for extinction effects.

Fig. 8 shows the averaged proportion of chemical components to extinction coefficient in PM_{10} during the CAREBeijing 2006 campaign under (a) clean and (b) hazy days. Ammonium sulfate, ammonium nitrate, organic mass, elemental carbon and coarse mass accounted for 26.5%, 15.2%, 21.8%, 16.1% and 20.4% of the total extinction coefficient during clean days, and44.6%, 22.3%, 13.6%, 10.8% and 8.7% during hazy days. Ammonium sulfate, ammonium nitrate and POM accounted for 20.2%, 11.2% and 15.8% of the mass concentration of PM_{10} during clean days, and 34.0%, 19.1% and 13.9% during hazy days (Han *et al.*, 2013). Obviously, ammonium sulfate was the largest contribution to the total extinction coefficient, which was comparable to other cities like Hong Kong (47%) (Cheung *et al.*, 2005), Jinan (41%) (Yang *et al.*, 2007), and Guangzhou (40.1%) (Tao *et al.*, 2009) in China and eastern United States (40%) (Watson, 2002). However, organic mass was the largest contributor to the total extinction coefficient in Xiamen (Zhang *et al.*, 2012). The proportion of ammonium sulfate and ammonium nitrate were significantly higher during the hazy time than that during the clean days. While the contribution of organic mass, elemental carbon and coarse mass were lower during the hazy time than that during the clean days. It was characterized that $(NH_4)_2SO_4 + NH_4NO_3$ increased while carbonaceous material decreased from clean days to hazy days (Fig. 8), which implied that the SNA (sulfate, nitrate, and ammonium) pollutants were more important than carbonaceous pollution for haze formation, and the problem of secondary pollution for haze episodes was mainly SNA pollution in Beijing.

CONCLUSIONS

As a part of the CAREBeijing 2006 campaign which was carried out from 18 August to 8 September, 2006, aerosol optical and physical properties as well as the aerosol chemical components were observed simultaneously. In this study, we analyzed the characteristics of the aerosol optical properties and explored the relations to the change of the chemical components.

During haze conditions, the averaged concentrations of SO_4^{2-}, NO_3^-, NH_4^+ and POM were 49.8, 31.4, 25.8 and

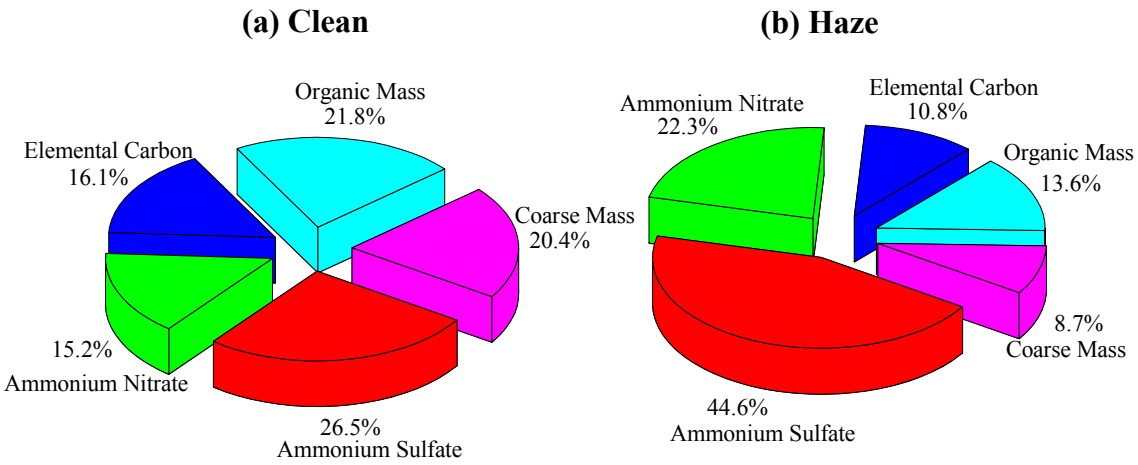

Fig. 8. The averaged fractional contributions to extinction coefficient by chemical components under (a) Clean day, and (b) Hazy day during the CAREBeijing 2006 campaign.

25.0 μg/m^3 respectively, which were significantly higher than the overall averaged conditions during the campaign (34.8, 24.5, 20.7 and 20.9 μg/m^3), and much higher than that of the clean days (11.7, 9.2, 6.3 and 13.9 μg/m^3). Pronounced diurnal cycles were observed for ω_{550}, b_{sp}, b_{ap} and b_{ext}. The dry b_{sp} was elevated during the daytime with a maximum mean value of 475.8 Mm^{-1} (LST 06:00). Both the mean and median values then fell below one between LST 08:00 and LST 20:00 with a minimum mean value of 120 Mm^{-1} (LST 20:00). The b_{ext} value increased at night probably due to the lower nocturnal boundary layer while surface emissions continued, and then decreased during the daytime due to the uplift of the boundary layer. The diurnal variations of $PM_{2.5}$ mass concentration and $PM_{2.5}/PM_{10}$ ratio were consistent with the b_{ext}. The b_{ap} value increased at night, and decreased during the daytime and reached the minimum (37 Mm^{-1}) at LST 16:00. The single scattering albedo reached its maximum at LST 11:00. This trend was consistent with the SNA/PM_{10} ratio and was contrary to the BC (black carbon)/PM_{10} ratio, which demonstrated that secondary pollution largely influenced the scattering ability of aerosol cluster and the chemical composition had an important impact on the aerosols optical properties. In addition, the diurnal variations of SOR and NOR further confirmed the influence of secondary pollutants on SSA.

The b_{ext}, b_{ap} and b_{sp} showed an increasing trend with $PM_{2.5}$ mass concentration and the correlation coefficient were 0.90, 0.95 and 0.98, respectively. The calculated b_{ext} by the modified IMPROVE algorithm agreed with the measured b_{ext} and the correlation coefficient between measured b_{ext} and calculated b_{ext} was 0.92. Ammonium sulfate, ammonium nitrate, organic mass, elemental carbon and coarse mass accounted for 26.5%, 15.2%, 21.8%, 16.1% and 20.4% of the total extinction coefficient during clean days, and accounted for 44.6%, 22.3%, 13.6%, 10.8% and 8.7% during hazy days. It is obvious that ammonium sulfate was the largest contributor to the total extinction coefficient. The proportion of ammonium sulfate and ammonium nitrate were apparently higher during the hazy time than that during the clean day. While the contribution of organic mass, elemental carbon and coarse mass were lower during the hazy time than that during the clean day, which implied that the SNA (sulfate, nitrate, and ammonium) pollutants were more important than carbonaceous pollution for haze formation, and the problem of secondary pollution for haze episodes was mainly SNA pollution in Beijing.

ACKNOWLEDGMENT

This work was supported by the Ministry of Science and Technology of China (Grant No. 2013CB955804), the National Natural Science Foundation of China (Grant No. 41005063 and No. 41175018) and the special fund of State Key Joint Laboratory of Environment Simulation and Pollution Control (No. 13Z02ESPCP and No. 13K04ESPCP).

REFERENCE

Alados-Arboledas, L., Alcántara, A., Olmo, F.J., Martínez-Lozano, J.A., Estellés, V., Cachorro, V., Silva, A.M., Horvath, H., Gangl, M., Díaz, A., Pujadas, M., Lorente, J., Labajo, A., Sorribas, M. and Pavese, G. (2008). Aerosol Columnar Properties Retrieved from CIMEL Radiometers during VELETA 2002. *Atmos. Environ.* 42: 2654–2667.

Anderson, T.L. and Ogren, J.A. (1998). Determining Aerosol Radiative Properties Using the TSI 3563 Integrating Nephelometer. *Aerosol Sci. Technol.* 29: 57–69.

Andreae, M.O., Schmid, O., Yang, H., Chand, D., Yu, J.Z., Zeng, L.M. and Zhang, Y.H. (2008). Optical Properties and Chemical Composition of the Atmospheric Aerosol in Urban Guangzhou, China. *Atmos. Environ.* 42: 6335–6350.

Bergin, M.H., Cass, G.R., Xu, J., Fang, C., Zeng, L.M., Yu, T., Salmon, L.G., Kiang, C.S., Tang, X.Y., Zhang, Y.H. and Chameides, W.L. (2001). Aerosol Radiative, Physical, and Chemical Properties in Beijing during June 1999. *J. Geophys. Res.* 106: 17969–17980.

Bokoye, A.I., Royer, A., O'Neill, N.T., Fedosejevs, G., Teillet, P.M. and McArthur, B. (2001). Characterization

of Atmospheric Aerosols across Canada. Assessment from a Ground-based Sunphotometer Network: AEROCAN. *Atmos. Ocean* 39: 429–456

Campanelli, M., Estellés, V., Tomasi, C., Nakajima, T., Malvestuto, V. and Martínez-Lozano, J.A. (2007). Application of the SKYRAD Improved Langley Plot Method for the in Situ Calibration of CIMEL Sun-sky Photometers. *Appl. Opt.* 46: 2688–2702.

Chan, Y.C., Simpson, R.W., Mctainsh, G.H., Vowles, P.D., Cohen, D.D. and Bailey, G.M. (1999). Source Apportionment of Visibility Degradation Problems in Brisbane (Australia) Using the Multiple Linear Regression Techniques. *Atmos. Environ.* 33: 3237–3250.

Cheng, Y.F., Wiedensohler, A., Eichler, H., Su, H., Gnauk, T., Brüggemann, E., Herrmann, H., Heintzenberg, J., Slanina, J., Tuch, T., Hu, M. and Zhang, Y.H. (2008). Aerosol Optical Properties and Related Chemical Apportionment at Xinken in Pearl River Delta of China. *Atmos. Environ.* 42: 6351–6372.

Cheung, H.C., Wang, T., Baumann, K. and Guo, H. (2005). Influence of Regional Pollution Outflow on the Concentrations of Fine Particulate Matter and Visibility in the Coastal Area of Southern China. *Atmos. Environ.* 39: 6463–6474.

Chýlek, P. and Wong, J. (1995). Effect of absorbing Aerosols on Global Radiation Budget. *Geophys. Res. Lett.* 22: 929–931.

Duan, F.K., He, K.B., Ma, Y.L., Yang, F.M., Yu, X.C., Cadle, S.H., Chan, T. and Mulawa, P.A. (2006). Concentration and Chemical Characteristics of $PM_{2.5}$ in Beijing, China: 2001–2002. *Sci. Total Environ.* 355: 264–275.

Garland, R., Schmid, O., Nowak, A., Achtert, P., Wiedensohler, A., Gunthe, S.S., Takegawa, N., Kita, K., Kondo, Y., Hu, M., Shao, M., Zeng, L.M., Zhu, T., Andreae, M.O. and Pöschl, U. (2008). Aerosol Optical Properties in a Rural Environment near the Mega-city Guangzhou, China: Implications for Regional Air Pollution, Radiative Forcing and Remote Sensing. *Atmos. Chem. Phys.* 8: 5161–5186.

Goloub, P., Li, Z., Dubovik, O., Blarel, L., Podvin, T., Jankowiak, I., Lecoq, R., Deroo, C., Chatenet, B., Morel, J.P., Cuevas, E. and Ramos, R. (2008). PHOTONS/ AERONET Sunphotometer Network Overview: Description, Activities, Results, Fourteenth International Symposium on Atmospheric and Ocean Optics/Atmospheric Physics, Matvienko, G.G. and Banakh, V.A. (Eds.), Proceedings of the SPIE, Volume 6936, Article ID. 69360V, 15 pp.

Gu, J.X., Bai, Z.P., Li, W.F., Wu, L.P., Liu, A.X., Dong, H.Y. and Xie, Y.Y. (2011). Chemical Composition of $PM_{2.5}$ during Winter in Tianjin, China. *Particuology* 9 215–221.

Han, T.T., Liu, X.G., Zhang, Y.H., Qu, Y., Ma, Q., Tian, H.Z., Zeng, L.M., Hu, M. and Zhu, T. (2013). The Role of Secondary Aerosols on Haze Formation in Summer in the Megacity Beijing, China. *Atmos. Environ.* Submitted.

He, K.B., Yang, F.M., Ma, Y.L., Zhang, Q., Yao, X.H., Chan, C.K., Cadle, S., Chan, T. and Mulawa, P. (2001). The Characteristics of $PM_{2.5}$ in Beijing, China. *Atmos. Environ.* 35: 4959–4970.

Holben, B.N., Eck, T.F., Slutsker, I., Tanre, D., Buis, J.P., Setzer, A., Vermote, E., Reagan, J.A., Kaufman, Y.J., Nakajima, T., Lavenu, F., Jnnkowiak, I. and Smirnov, A. (1998). AERONET – A Federated Instrument Network and Data Archive for Aerosol Characterization. *Remote Sens. Environ.* 66: 1–16.

IPCC (2007). Summary for Policymakers, In *Climate Change 2007: The Physical Science Basis. Contribution of Working Group I to the Fourth Assessment Report of the Intergovernmental Panel on Climate Change*, Solomon, S., Qin, D., Manning, M., Chen, Z., Marquis, M., Averyt, K.B., Tignor, M. and Miller, H.L. (Eds.), Cambridge University Press, Cambridge, United Kingdom and New York, NY, USA.

Kondo, Y., Komazaki, Y., Miyazaki, Y., Moteki, N., Takegawa, N., Kodama, D., Deguchi, S., Nogami, M., Fukuda, M., Miyakawa, T., Morino, Y., Koike, M., Sakurai, H. and Ehara, K. (2006). Temporal Variations of Elemental Carbon in Tokyo. *J. Geophys. Res.* 111, D12205, doi: 10.1029/2005JD006257.

Li, C., Marufu, L.T., Dickerson, R.R., Li., Z., Wen, T., Wang, Y., Wang, P., Chen, H. and Stehr, J.W. (2007). In Situ Measurements of Trace Gases and Aerosol Optical Properties at a Rural site in Northern China during East Asian Study of Tropospheric Aerosols: An International Regional Experiment 2005. *J. Geophys. Res.* 112: D22S04, doi: 10.1029/2006JD007592.

Li, Y., Demetriades-Shah, T.H. Kanemasu, E.T., Shultis, J.K. and Kirkham, M.B. (1993). Use of Second Derivatives of Canopy Reflectance for Monitoring Prairie Vegetation over Different Soil Backgrounds. *Remote Sens. Environ.* 44: 81–87.

Liu, X.G., Cheng, Y.F., Zhang, Y.H., Jung, J.S., Sugimoto, N., Chang, S.Y., Kim, Y.J., Fan, S.J. and Zeng, L.M. (2008). Influences of Relative Humidity and Particle Chemical Composition on Aerosol Scattering Properties during The 2006 PRD Campaign. *Atmos. Environ.* 42: 1525–1536.

Liu, X.G., Zhang, Y.H., Jung, J.S., Gu, J.W., Li, Y.P., Guo, S., Chang, S.Y., Yue, D., Lin, P., Kim, Y.J., Hu, M., Zeng, L.M. and Zhu, T. (2009). Research on Aerosol Hygroscopic Properties by Measurement and Model during the 2006 CAREBeijing Campaign. *J. Geophys. Res.* 114: D00G16, doi: 10.1029/2008JD010805.

Liu, X.G., Zhang, Y.H., Cheng, Y.F., Hu, M. and Han, T.T. (2012). Aerosol Hygroscopicity and Its Impact on Atmospheric Visibility and Radiative Forcing in Guangzhou during the 2006 PRIDE-PRD Campaign. *Atmos. Environ.* 60: 59–67.

Liu, X.G., Gu, J.W., Li, Y.P., Cheng, Y.F., Qu, Y., Han, T.T., Wang, J.L., Tian, H.Z., Chen, J. and Zhang, Y.H. (2013a). Increase of Aerosol Scattering by Hygroscopic Growth: Observation, Modeling, and Implications on Atmospheric Visibility. *Atmos. Res.* 132–133: 91–101.

Liu, X.G., Li, J., Qu, Y., Han, T.T., Hou, L., Gu, J.W., Chen, C., Yang, Y.R., Liu, X.Y., Yang, T., Zhang, Y.H., Tian, H.Z. and Hu, M. (2013b). Formation and Evolution Mechanism of Regional Haze: A Case Study in Mega-city Beijing of China. *Atmos. Chem. Phys.* 13: 4501–4514.

Malm, W.C. and Persha, G. (1991). Considerations in the

Accuracy of a Long-path Transmissiometer. *Aerosol Sci. Technol.* 14: 459–471.

Malm, W.C., Sisler, J.F., Huffman, D., Eldred, R.A. and Cahill, T.A. (1994). Spatial and Seasonal Trends in Particle Concentration and Optical Extinction in the United States. *J. Geophys. Res.* 99: 1347–1370.

Malm, W.C. and Day, D.E. (2001). Estimates of Aerosol Species Scattering Characteristics as a Function of Relative Humidity. *Atmos. Environ.* 35: 2845–2860.

Malm, W.C. and Hand, J.L. (2007). An Examination of the Physical and Optical Properties of Aerosols Collected in the IMPROVE Program. *Atmos. Environ.* 41: 3407–3427.

Molina, M.J. and Molina, L.T. (2004). Megacities and Atmospheric Pollution. *J. Air Waste Manage. Assoc.* 54: 644–680.

O'Brien, D.M. and Mitchell, R.M. (2003). Atmospheric Heating due to Carbonaceous Aerosol in Northern Australia-confidence Limits Based on TOMS Aerosol Index and Sun-photometer Data. *Atmos. Res.* 66: 21–41.

Orsini, D.A., Ma, Y., Sullivan, A., Sierau, B., Baumann, K. and Weber, R.J. (2003). Refinements to the Particle-into-liquid Sampler (PILS) for Ground and Airborne Measurements of Water Soluble Aerosol Composition. *Atmos. Environ.* 37: 1243–1259.

Petzold, A. and Schonlinner, M. (2004). Multi-angle Absorption Photometry-A New Method for the Measurement of Aerosol Light Absorption and Atmospheric Black Carbon. *J. Aerosol Sci.* 35: 421–441.

Strawbridge, K.B. and Snyder, B.J. (2004). Planetary Boundary Layer Height Determination during Pacific 2001 Using the Advantage of a Scanning Lidar Instrument. *Atmos. Environ.* 38: 5861–5871,

Sugimoto, N., Nishizawa, T., Liu, X.G., Matsui, I., Shimizu, A., Zhang, Y.H., Kim, Y.J., Li, R. H. and Liu, J. (2009). Continuous Observations of Aerosol Profiles with a Two-wavelength Mie-scattering Lidar in Guangzhou in PRD2006. *J. Appl. Meteor. Climatol.* 48: 1822–1830.

Sun, Y.L., Zhuang, G.S., Tang, A.H., Wang, Y. and An, Z.S. (2006). Chemical Characteristics of $PM_{2.5}$ and PM_{10} in Haze-Fog Episodes in Beijing. *Environ. Sci. Technol.* 40: 3148–3155.

Tan, J.H., Duan, J.C., He, K.B., Ma, Y.L., Duan, F.K., Chen, Y. and Fu, J.M. (2006). Chemical Characteristics of $PM_{2.5}$ during a Typical Haze Episode in Guangzhou. *J. Environ. Sci.* 21: 774–781.

Tao, J., Ho, K.F., Chen, L.G., Zhu, L.H., Han, J.L. and Xu, Z.C. (2009). Effect of Chemical Composition of $PM_{2.5}$ on Visibility in Guangzhou, China, 2007 Spring. *Particuology* 7: 68–75.

Turpin, B.J. and Lim, H.J. (2001). Species Contributions to $PM_{2.5}$ Mass Concentrations: Revisiting Common Assumptions for Estimating Organic Mass. *Aerosol Sci. Technol.* 35: 602–610.

Uchiyama, A., Yamazaki, A., Togawa, H. and Asano, J. (2005). Characteristics of Aeolian Dust Observed by Sky-radiometer in the Intensive Observation Period 1 (IOP1). *J. Meteor. Soc. Japan* 83A: 291–305.

Wang, T. (2003). Study of Visibility and Its Causes in Hong Kong, The Environmental Protection Department of Hong Kong.

Watson, J.G. (2002). Visibility: Science and Regulation. *J. Air Waste Manage. Assoc.* 52: 628–713.

Wu, D., Bi, X., Deng, X., Li, F., Tan, H., Liao, G. and Huang, J. (2006). Effects of Atmospheric Haze on the Deterioration of Visibility over the Pearl River Delta. *Acta Meteorol. Sin*. 64: 510–517.

Xu, J., Bergin, M.H., Yu, X., Liu, G., Zhao, J., Carrico, C.M. and Baumann, K. (2002). Measurement of Aerosol Chemical, Physical and Radiative Properties in the Yangtze Delta Region of China. *Atmos. Environ.* 36: 161–173.

Yan, P., Tang, J., Huang, J., Mao, J.T., Zhou, X.J., Liu, Q., Wang, Z.F. and Zhou, H.G. (2008). The Measurement of Aerosol Optical Properties at a Rural Site in Northern China. *Atmos. Chem. Phys.* 7: 2229–2242.

Yang, F., He, K., Ye, B., Chen, X., Cha, L., Cadle, S.H., Chan, T. and Mulawa, P.A. (2005). One-year Record of Organic and Elemental Carbon in Fine Particles in Downtown Beijing and Shanghai. *Atmos. Chem. Phys.* 5: 1449–1457.

Yang, L.X., Wang, D.C., Cheng, S.H., Wang, Z., Zhou, Y., Zhou, X.H. and Wang, W.X. (2007). Influence of Meteorological Conditions and Particulate Matter on Visual Range Impairment in Jinan, China. *Sci. Total Environ.* 383: 164–173.

Yao, X.H., Chan, C.K., Fang, M., Cadle, Chan, S.T., Mulawa, P., He, K.B. and Ye, B.M. (2002). The Water-soluble Ionic Composition of $PM_{2.5}$ in Shanghai and Beijing. China. *Atmos. Environ.* 36: 4223–4234.

Ye, B.M., Ji, X.L., Yang, H.Z., Yao, X.H., Chan, C.K., Cadle, S.H., Chan, T. and Mulawa, P.A. (2003). Concentration and Chemical Composition of $PM_{2.5}$ in Shanghai for a 1-year Period. *Atmos. Environ.* 37: 499–510.

Yuan, C.S., Lee, C.G., Liu, S.H., Chang, J.C., Yuan, C. and Yang, H.Y. (2006). Correlation of Atmospheric Visibility with Chemical Composition of Kaohsiung Aerosols. *Atmos. Res.* 82: 663–679.

Zhang, F.W., Xu, L.L., Chen, J.S., Yu, Y.K., Niu, Z.C. and Yin, L.Q. (2012). Chemical Compositions and Extinction Coefficients of $PM_{2.5}$ in Peri-urban of Xiamen, China, during June 2009-May 2010. *Atmos. Res.* 106: 150–158.

Received for review, June 20, 2013
Accepted, September 30, 2013